A novel σ-linkage to dianchor dyes for efficient dyes sensitized solar cells: 3-methyl-1,1-cyclohexane

Isolda Duerto [a]§, Marta García-Palacín [a]§, Daniel Barrios[b], Javier Garín[a], Jesús Orduna[a], Belén Villacampa[b], María-J. Blesa [a]*

Addresses:

[a] Departamento de Química Orgánica, ICMA
Universidad de Zaragoza-CSIC
50009, Zaragoza (Spain)
E-mail: mjblesa@unizar.es

[b] Departamento de Física de la Materia Condensada, ICMA
Universidad de Zaragoza-CSIC
50009, Zaragoza (Spain)

§: Both authors contributed equally to this work.

Corresponding author:

Dr. María-Jesús Blesa: mjblesa@unizar.es

Authors:

Isolda Duerto: isolda@unizar.es
Marta García-Palacín: martagarciapalacin@gmail.com
Daniel Barrios: 790772@unizar.es
Prof. Javier Garín: jgarin@unizar.es
Dr. Jesús Orduna: jorduna@unizar.es
Dr. Belén Villacampa: bvillaca@unizar.es
Dr. María-Jesús Blesa: mjblesa@unizar.es

Declarations of interest: none

Keywords
Aggregation; dye; metal-free sensitizer; multichromophore; temporal stability

A novel σ-linkage to dianchor dyes for efficient dyes sensitized solar cells: 3-methyl-1,1-cyclohexane

Abstract

We have synthesized two sensitizers based on the 3-methyl-1,1-cyclohexane, a novel σ-linkage to prepare dianchored dyes. These novel dyes are difunctionalized systems with aniline-donor (D), a π-conjugated spacer (π) based on thiophene or bithiophene and cyanoacetic acid as acceptor and anchoring group (A). The UV-vis absorption and the Differential Pulse Voltammetry have been used to study the effect of both σ-linkage and π-spacer. The relevant increase of the molar extinction coefficient of these dianchored dyes has been investigated by theoretical calculations. The dye bearing bithiophene results in a both broader and higher absorption as well as an adequate efficiency to transfer charge from D to A with respect to bithiophene dyes. The photovoltaic properties of these sensitizers without co-adsorbent have been studied. The novel difunctionalized derivatives present a relevant increase of the photocurrent density which results in a better performance with respect to the single dyes. The difunctionalized derivative based on bithiophene has given rise to an efficiency value of 7.8 % and is stable up to 1000 h after the device assembly.

TABLE OF CONTENTS

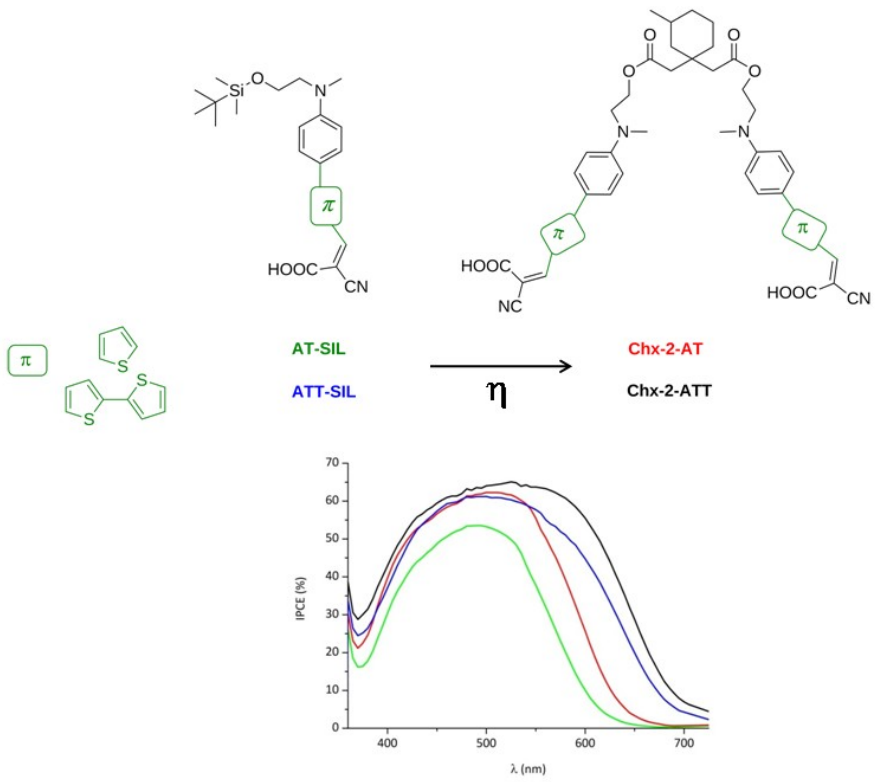

1. Introduction

Gratzel cells or Dye Sensitized Solar Cells (DSSCs)[1] are always able to enlarge the materials market with others lighter and more flexible which might be used to design wireless self-powering devices to be used indoor and outdoor.[2-4] These DSSCs include an anode made of a wide-bandgap semiconductor with anchored dye molecules, a counter electrode and a redox mediator[1]. The dye is likely the fundamental element because it is responsible of both harvesting the solar light and generating electrons to be injected into the photoanode.

Dye sensitizers are commonly formed by a D-π-A structure and organic synthesis makes them easy to prepare.[5] They are free of metals and, consequently, environmentally friendly. [6-7] As the development of different triarylamine sensitizers has given promising efficiencies, [8,9] further structural modifications of aniline moiety, a good electron donor (D), seems a natural step forward. The π-bridge structure can be used to tune the photochemical properties of the organic dye. [10-13] In particular, it is usually designed to broaden the absorption to make them more effective for the sun light spectrum[14] as well as to provide chemical stability[15] to the sensitizer. Recently, a novel dyes based on a ruthenium-diacetylide structure [4] and functionalized triphenylamine-dyes all bearing functionalized bithiophene as π-bridge were studied and exhibited promising power conversion efficiencies [16-17]. Lastly, DSSC-sensitizers mainly use the cyanoacrylic acid because the presence of the cyano group, an electron withdrawing group (A), close to the carboxylic acid group, which acts as anchoring, produce an adequate intramolecular charge transfer (ICT) as well as a good electron injection.

It is also described in the literature how dyes with various anchoring points and adequate arrangements of the D-π-A systems provide, in general, improved photovoltaic properties. Different strategies have been followed to enhance the optical density and binding strength of dyes onto titanium particles [18] such as dianchored sensitizers with both donor parts linked by a π-spacer [17] and dyes with several acceptor units linked by a common donor part. [19] In particular, Su *et al.* introduced one, two and three thiophene segments into calix[4]arene based dyes to form cone-shaped structures with four chromophores, which offered decreased aggregation, lower charge recombination and temporal stability. [20] In general, an improvement of the overall efficiency can be achieved through broadening the absorption spectrum and increasing both the light harvesting efficiency of the dye and the sensitizer loading of the photoanode.[21] In our research group we have prepared sensitizers connected through a σ-linker and it has been proved that the introduction of several dyes in a scaffold allows increasing the distance between the chromophore groups avoiding their interaction[22] and, at the same time, the extinction coefficient is increased, allowing the device to work in conditions of low luminosity. [23,24]

The goal of this paper is to study the properties of difunctionalized dyes based on a novel σ-linkage, the 3-methyl-1,1-cyclohexane, with two chromophores, which are constituted by *N, N*-dialkylaniline as donor (D), thiophene or bithiophene as π-spacer (π) and a cyanoacetic group as acceptor (A) and anchoring group. The effect of this σ-linkage on the physical properties and photovoltaic performances of these double dyes will be evaluated and compared with those of the corresponding single D-π-A structure. Moreover, the influence of the introduction of a second thiophene in the π-spacer will be also analyzed.

2. Results and Discussion

2.1. Synthesis and Characterization

Chart 1 depicts the structures of compounds **AT-SIL, ATT-SIL, Chx-2-AT** and **Chx-2-ATT.** The monoanchored dye **AT-SIL** [25] is used as reference and it is used to evaluate the properties of the dye with two thiophenes as π-spacer, **ATT-SIL ,**and the dianchored dyes, **Chx-2-AT** and **Chx-2-ATT,** with two chromophores in the same structure.

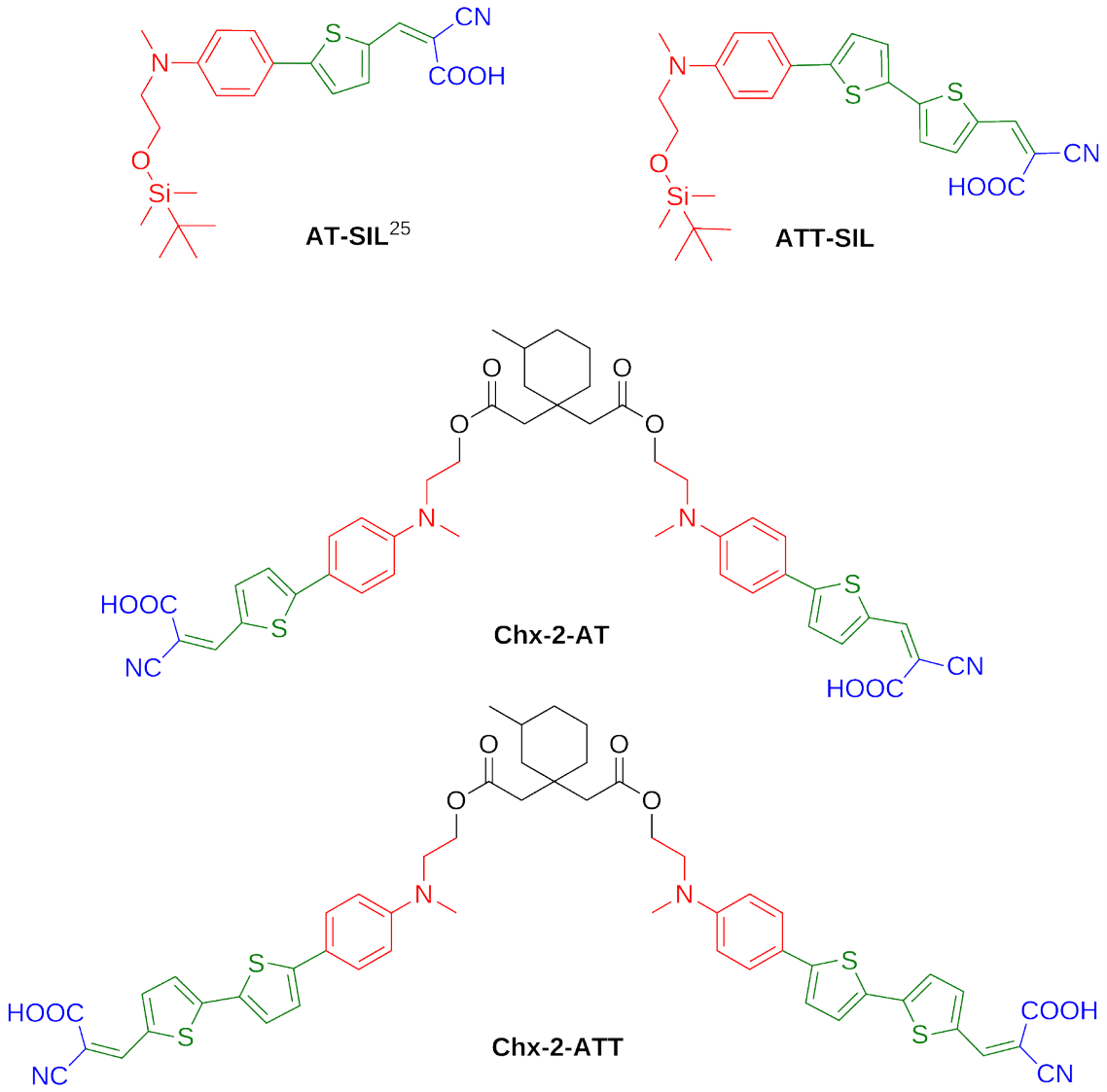

Chart 1. Dyes **AT-SIL, ATT-SIL, Chx-2-AT** and **Chx-2-ATT**

Scheme 1 shows the preparation of aldehydes **3**[26] and **4**. The donor part was synthesized according to Duerto *et al*. [25] Particularly, it was prepared by bromination of *N*-methyl-*N*-(2-hydroxyethyl)aniline. *Tert*-butyldimethylsilyl chloride was used as protective reagent to functionalize the alcohol group of the starting aniline. Then the Stille reaction was carried out. The coupling of the organostannane with the corresponding organic electrophiles, 5-bromothiophen-2-carbaldehyde or 5-bromo-[2,2'-bithiophene]-5-carbaldehyde[27] was carried out via Stille palladium catalyzed coupling reaction[28] to give aldehydes **1**[25] and **2**, respectively. At last, the desired compounds **3** and **4** were obtained after removing the *tert*-butyldimethylsilyl group of the aldehydes **1** and **2** with tetrabutylammonium fluoride (TBAF) in anhydrous tetrahydrofuran (THF) at room temperature.

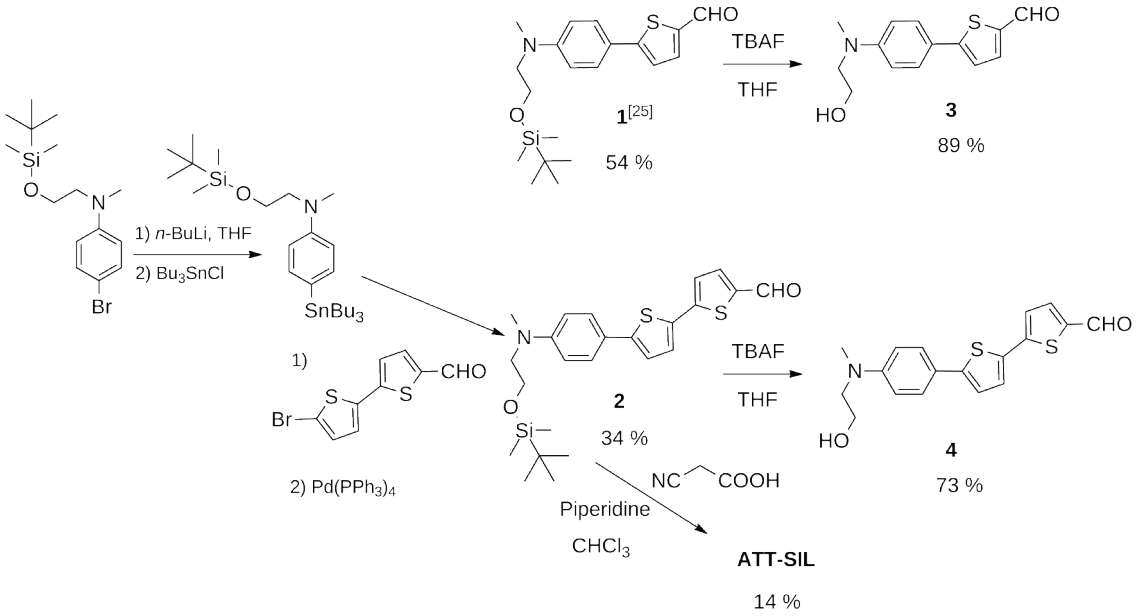

Scheme 1. Preparation of compounds **3, 4** and **ATT-SIL**

The dye **ATT-SIL** was prepared in basic media by Knoevenagel reaction of the aldehyde **2** with cyanoacetic acid (**Chart 1**).

Scheme 2 shows the preparation of the dianchored dyes **Chx-2-AT** and **Chx-2-ATT**. Dialdehydes **5** and **6** were synthesized according to the procedure described in the literature[23] from 3-methyl-1,1-cyclohexanediacetic acid using 1-ethyl-3-(3-dimethylaminopropyl)carbodiimide (EDC) by a Steglich reaction of compounds **3** and **4**, respectively. Finally, the formyl group of dialdehydes **5** and **6** reacted with cyanoacetic acid in basic media by a Knoevenagel condensation and the dianchored **Chx-2-AT** and **Chx-2-ATT** were obtained (**Chart 1**).

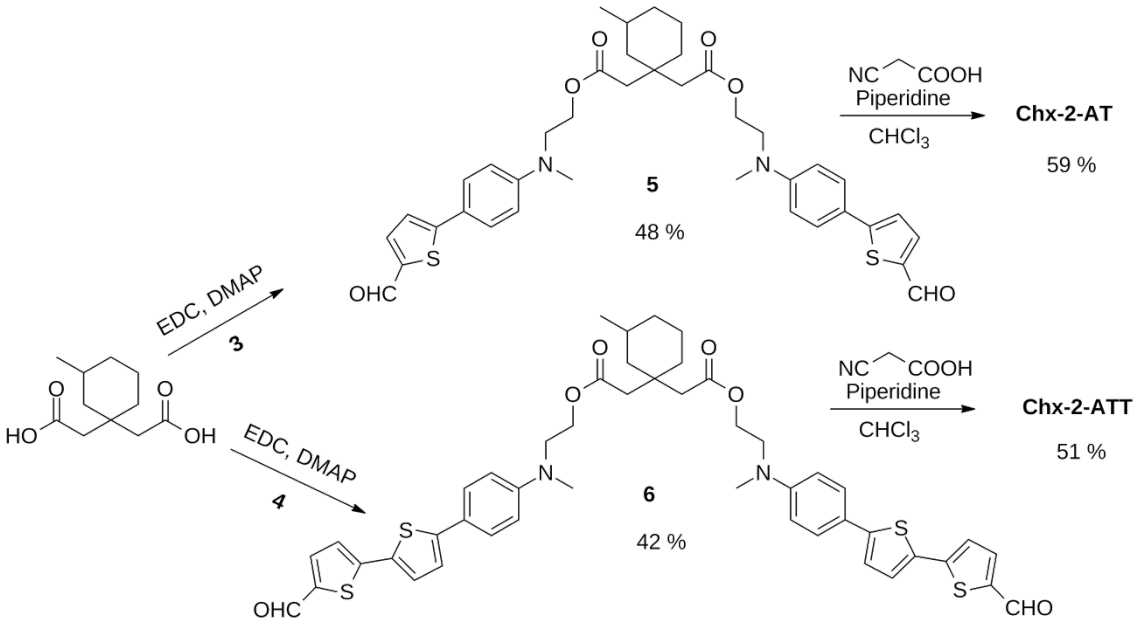

Scheme 2. Preparation of the dyes **Chx-2-AT** and **Chx-2-ATT**

2.2. Optical properties

The UV–vis absorption of the sensitizers **AT-SIL** [25]**, ATT-SIL, Chx-2-AT** and **Chx-2-ATT** have been measured in tetrahydrofurane solution (10^{-5} M, **Figure 1**), and on the corresponding sensitized TiO_2 films (**Figure 2**).

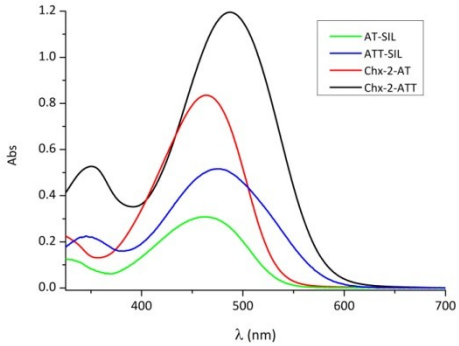

Figure 1. UV–vis absorption spectra of **AT-SIL, ATT-SIL, Chx-2-AT** and **Chx-2-ATT** in THF solution.

The spectra of **AT** derivatives (**AT-SIL** and **Chx-2-AT**) in solution show a band (370–550 nm) in the visible region, which, according to DFT calculations (section 2.4), can be attributed to the intramolecular charge transfer (ICT) between the electron-withdrawing and the electron-donating moieties of chromophores. The spectra of **ATT** derivatives (**ATT-SIL** and **Chx-2-ATT**) show at 350 nm a band, which is assigned to a π → π* electronic transition, whereas at lower energy, an ICT band (400-600 nm) is observed.

Table 1 collects the optical properties of **AT-SIL, ATT-SIL, Chx-2-AT** and **Chx-2-ATT.**

Table 1. Optical parameters of dyes **AT-SIL, ATT-SIL, Chx-2-AT** and **Chx-2-ATT**

Dye	λ_{abs} [a] **(nm)**	λ_{abs} [b] **(nm)**	ε [a] **(10^4 M^{-1}·cm^{-1})**
AT-SIL	470	397	1.68±0.04
ATT-SIL	474	452	2.45±0.02
Chx-2-AT	464	424	4.35±0.06
Chx-2-ATT	487	436	6.18±0.14

[a]In THF solution (10^{-5} M). [b] Absorption on TiO_2 films.

The molar extinction coefficient (ε) of the difunctionalized dyes **Chx-2-AT** and **Chx-2-ATT** increases (roughly x 2.5) with respect to **AT-SIL** and **ATT-SIL,** respectively (Supporting Information, **Figures S.1-S.4**). The cyclohexane derivatives exhibit higher molar extinction coefficient values than expected, bearing in mind the absorption of single dyes. This result, which will be explained in section **2.4.**, points to the promising light-absorption ability of these double anchored sensitizers.

Figure 2 (normalized spectra) and **Figures S.5-S.8** (Supporting Information) show the UV spectra of the films of the adsorbed dyes on TiO_2. When these films are sensitized, a hypsochromic shift is observed in the corresponding spectra with respect to those in THF solution. Generally, the blue shifts can be attributed to the deprotonation of the dyes and/or the formation of *H*-aggregates [29] on the TiO_2 surface. An UV–vis absorption study of **ATT-SIL, Chx-2-AT** and **Chx-2-ATT** films have been carried out after different time intervals of immersion (30 min, 2h 30 min and 5h) and it can be said that there is not aggregation confirmation because there is not an increase of the width of the spectrum ICT band on increasing the immersion time. Besides, the broad bands of **ATT-**derivatives on TiO_2 point a promising light absorption.

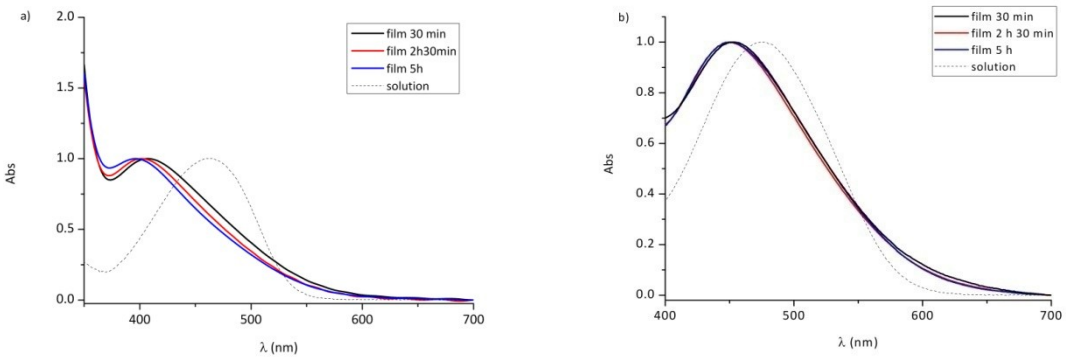

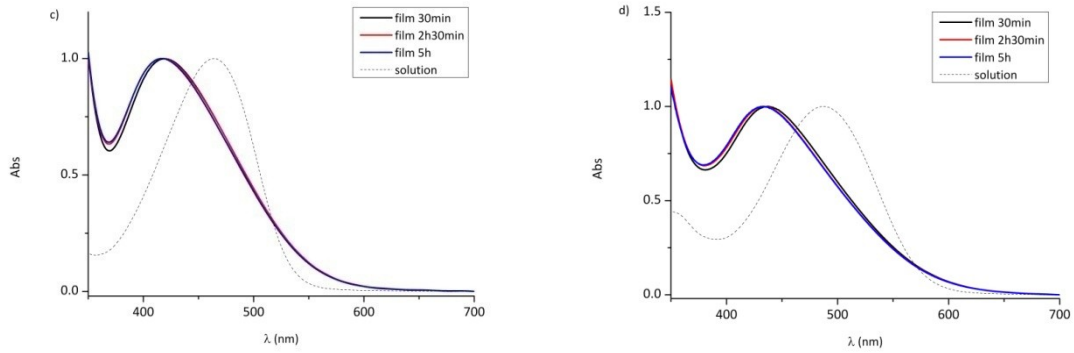

Figure 2. UV–vis spectra of films (_____) sensitized by a) **AT-SIL**, b) **ATT-SIL**, c) **Chx-2-AT**, d) **Chx-2-ATT** after 30 min, 2h30 and 5h of immersion. The normalized spectra of THF solution (———) are included for comparison.

2.3. Electrochemical properties

The voltamogramms of **AT-SIL[25], ATT-SIL, Chx-2-AT** and **Chx-2-ATT** were carried out by Differential Pulse Voltammetry (DPV) and Cyclic Voltammetry (CV). Dye solutions used was 5·10−4 M in THF. They are compiled in **Figures S.9-S.12** (Supporting Information). The oxidation process is reversible (Supporting Information). **Table 2** collects the oxidation potentials of both ground and excited states of these sensitizers.

Table 2. Electrochemical parameters: transition energy $E_{0\text{-}0}$ and potential values E_{ox} and E_{ox}^{*}

Dye	E_{ox} [a] (V)	$E_{0\text{-}0}$ [b] (eV)	E_{ox}^{*} [c] (V)
AT-SIL	+1.17	2.34	–1.17
ATT-SIL	+1.06	2.13	–1.14
Chx-2-AT	+1.20	2.32	–1.12
Chx-2-ATT	+1.07	2.14	–1.07

[a] The potential values were converted to normal hydrogen electrode (NHE) by addition of 0.199 V. [b] $E_{0\text{-}0}$ was estimated from the UV-vis spectra. [c] $E^*_{ox} = E_{ox} - E_{0\text{-}0}$.

In the area of Grätzel cells, dyes must comply with two electrochemical requirements. First, the E_{ox} value of the sensitizer (oxidation potential of the ground state) must be higher than the redox potential of the I_3^-/I^- electrolyte (+0.4 V [30]) to be sure that the sensitizer is regenerated after being oxidized. Second, the E_{ox}* value of the sensitizer (oxidation potential of the excited state) must be lower than the conduction band of TiO_2 (–0.5 V *vs* NHE [31]) to favor injection of electrons from the excited dye onto the photoanode. [32, 33] Sensitizers **AT-SIL** and **Chx-2-AT** have analogous E_{ox} values. This similarity is also observed with dyes **ATT-SIL** and **Chx-2-ATT** because they have the same π-spacer and donor moiety. The E_{ox} and E_{ox}* values of **AT-SIL, ATT-SIL, Chx-2-AT** and **Chx-2-ATT** point out that both electron injection and sensitizer regeneration are energetically favored. (Supporting Information, **Figure S.13**).

2.4. Theoretical calculations

By means of *DFT* (Density Functional Theory) calculations we can also characterize theoretically the optical and electrochemical properties of the dyes. First, we can consider the ground and first excited states of the dyes and their derived radical cations formed upon a one-electron oxidation. The optical parameters such as absorption wavelengths (λ_{abs}) and oscillator strengths (f) were computed on ground state geometries by TD-DFT (time dependent DFT). Furthermore, excitation energies ($E_{0\text{-}0}$) were calculated as the difference in Gibbs free energy between ground and excited states both at their equilibrium geometries. Analogously, the differences of

Gibbs free energy between neutral species and their oxidized radical cations allow us to estimate ground state oxidation potentials (E_{OX}) while those of the excited state were obtained as $E^*_{ox} = E_{ox} - E_{0\text{-}0}$. Results are presented on **Table 3**. It is noteworthy that calculated energies agree to experimental values within 0.2 eV.

Table 3. Results of DFT calculations.

Dye	λ_{abs}[a] (nm)	f	E_{HOMO} (eV)	E_{LUMO} (eV)	$E_{0\text{-}0}$ (eV)	E_{ox}[b] (V)	E^*_{ox}[b] (V)
AT-SIL[25]	434	1.11	-6.60	-2.08	2.45	1.19	-1.26
ATT-SIL	483	1.53	-6.43	-2.26	2.13	1.01	-1.11
Chx-2-AT	469	1.10	-6.52	-2.13	2.39	1.08	-1.30
	460	1.22					
Chx-2-ATT	502	1.95	-6.32	-2.30	2.17	1.10	-1.08
	495	1.05					

a) Calculated using equilibrium solvation. b) Referenced to normal hydrogen electrode (NHE).

TD-DFT calculations show that the lowest energy absorption of single-chromophore dyes **AT-SIL** and **ATT-SIL** is associated to a one-electron transition from the HOMO, located on the aryl amino donor moiety, to the LUMO located on the cyanoacetic acid acceptor (see **Figure 3**). The large HOMO-LUMO overlap over the bithiophene spacer accounts for the large oscillator strength associated to this transition. The presence of a second thiophene moiety on **ATT-SIL** causes a reduced HOMO-LUMO gap and increased oscillator strength compared to the single thiophene **AT-SIL** analogue.

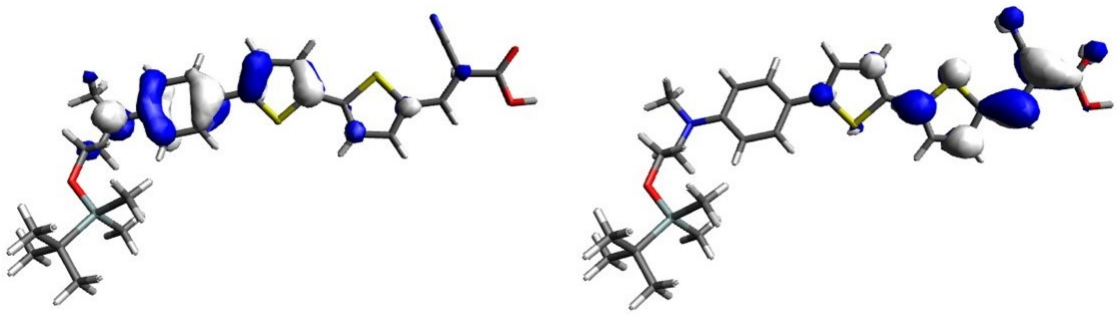

Figure 3. Contour plots for the HOMO (left) and LUMO (right) of **ATT-SIL** (0.04 isosurface value)

The electronic structure of dichromophoric dyes **Chx-2-AT** and **Chx-2-ATT** becomes more complicated. The HOMO levels in both chromophores combine giving rise to one symmetrical and one antisymmetrical orbital (HOMO-1 and HOMO) which are close in energy and in a similar way individual LUMOs combine to form LUMO and LUMO+1. (**Figure 4**)

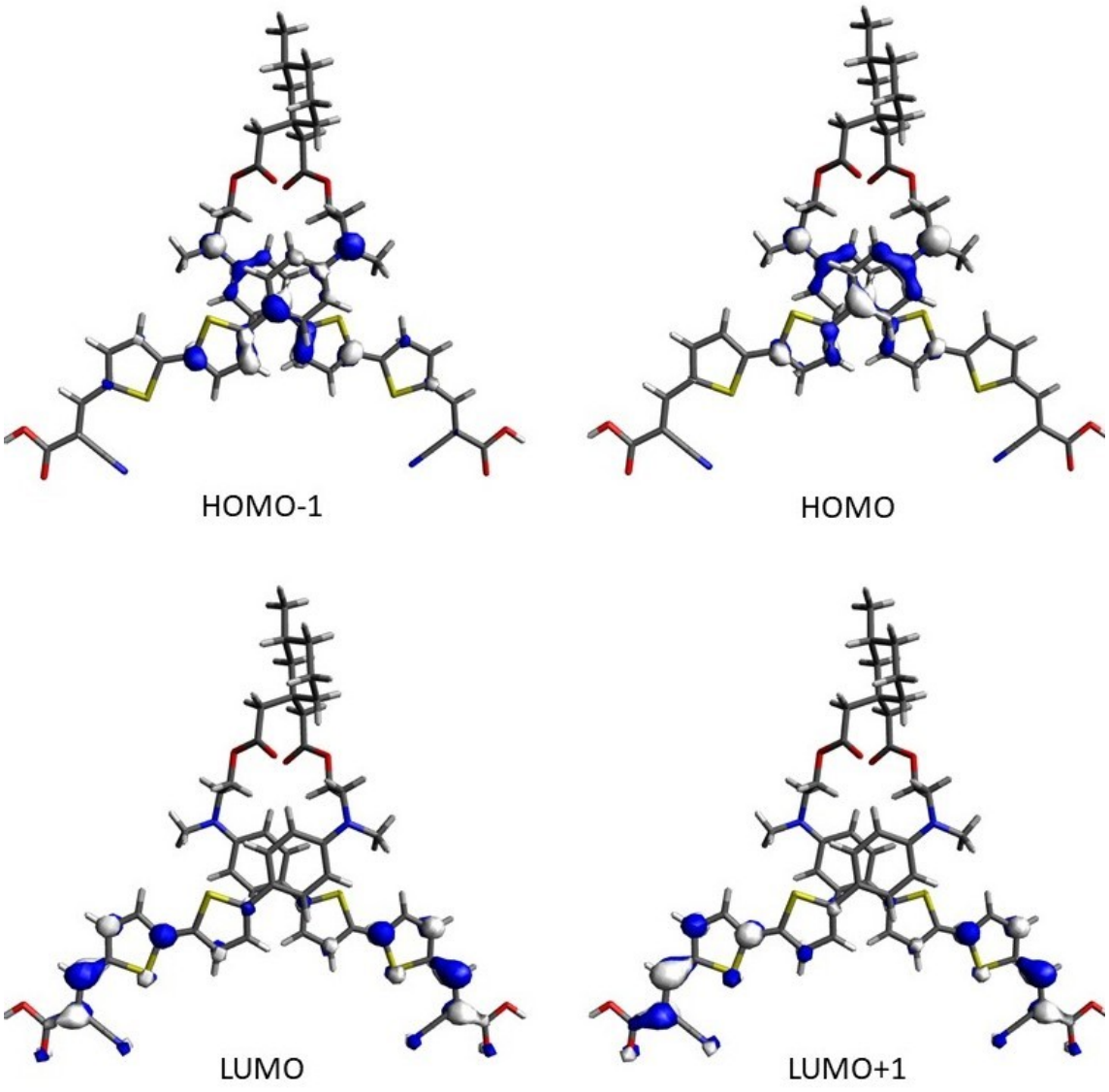

Figure 4. Contour plots for the molecular orbitals of **Chx-2-ATT** (0.04 isosurface value).

With this electronic structure, TD-DFT calculations predict two electronic transitions with very similar excitation energies. Taking **Chx-2-ATT** as example, the lowest energy absorption is calculated at 502 nm and is contributed from both a HOMO-1 to LUMO and a HOMO to LUMO+1 one electron transition and its calculated oscillator strength is higher than that of single-chromophore dyes due to its larger orbital extension. The next absorption, contributed from HOMO to LUMO and HOMO-1 to LUMO+1 transition, is calculated at 495 nm and also with large oscillator strength. Having in

mind that these absorptions are very close in energy, the experimental UV spectrum shows a large band that encompasses both absorptions with a large extinction coefficient (**Table 1**) that arises from the addition of their oscillator strengths and predicts a large Light Harvesting Efficiency (LHE).

We have also calculated the spin density plots of the oxidized radical cations for all the studied dyes (See **Figure 5**). A comparison to previously shown molecular orbitals indicates that upon oxidation the electron is extracted from the HOMO which is mainly located on the arylamine donor moiety. The low spin density on the acid group, which will be attached to the TiO_2 electrode in the assembled DSSC, accounts for an improbable Back Electron Transfer (BET) that could result in a decreased efficiency.

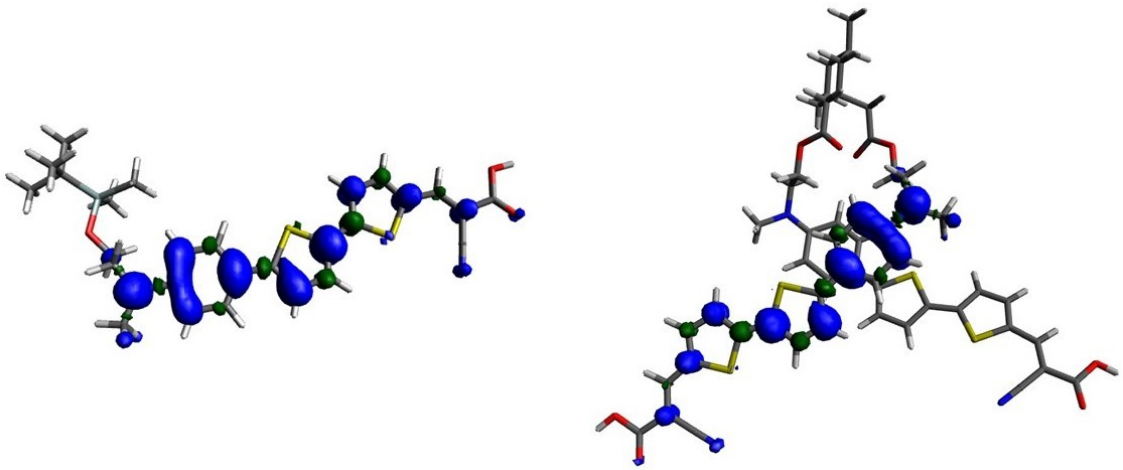

Figure 5. Spin density contour plots of radical cations of **ATT-SIL** (left) and **Chx-2-ATT** (right). (0.004 isosurface value).

2.5. Photovoltaic properties

A photovoltaic study of the DSSCs prepared with these dyes was carried out. The conditions for the preparation of the devices were compiled in Supporting Information (Section 2). Optimized devices were prepared with electrodes of 6 µm thick sensitized

with **AT-SIL, ATT-SIL, Chx-2-AT** and **Chx-2-ATT** dyes after 5 h of immersion time. **Figure 6** and **Table 4** collect the results acquired upon this photovoltaic characterization.

As concerns the comparison between thiophene (**AT-SIL, Chx-2-AT**) and bithiophene (**ATT-SIL** and **Chx-2-ATT**) based dyes, higher J_{sc} values have been measured for the cells incorporating bithiophene sensitizers. This result can be related with the better light harvesting ability of these systems, according with optical absorption results (**Figure 1** and **Figure S.5-S.8**). Regarding the voltage, the V_{oc} value is slightly higher for those double dyes as compared with the single dye counterparts (**Figure 6** (left), **Table 4**).

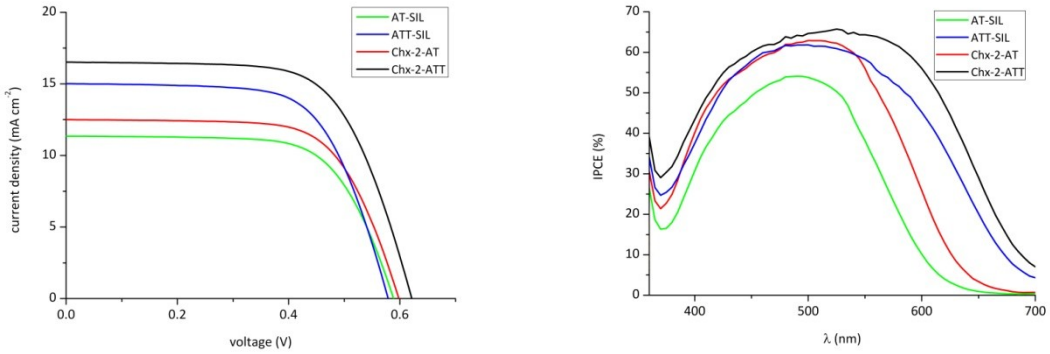

Figure 6. a) Current density vs voltage (left) (100 mW·cm^{-2}, under AM 1.5 G simulated solar light); b) IPCE spectra (right) for devices based on studied dyes (6 µm thick anodes, immersion time 5 h).

Figure 6 (right) depicts the incident photon to converted electron efficiency (IPCE) spectra. The comparison between thiophene and bithiophene based dyes shows a broader spectrum for the devices with bithiophene than those prepared with thiophene as it was expected taking into account the absorption of films (**Figure S.5-S.8**). Besides, the introduction of the novel σ-linkage gives rise to a better electron collection as compared with the corresponding single dyes. In summary, the device

prepared with dye **Chx-2-ATT** showed the broadest and highest IPCE spectrum in agreement with the higher J_{sc} value.

Table 4. Average value of the measured photovoltaic parameters: open circuit voltage (V_{oc}), short circuit current density (J_{sc}), fill factor (*ff*) and overall efficiency (η). Three cells of each type were prepared and characterized

Dye	Dye loading (mol·cm^{-2})	J_{sc} (mA cm^{-2})	V_{oc} (V)	*ff* (%)	η (%)
AT-SIL	$4.33\cdot10^{-7}$	11.351±0.331	0.589±0.005	67.48±0.13	4.48±0.17
ATT-SIL	$1.37\cdot10^{-7}$	15.011±0.062	0.579±0.006	65.78±0.63	5.70±0.14
Chx-2-AT	$1.06\cdot10^{-7}$	12.500±0.435	0.598±0.001	67.22±0.13	5.03±0.19
Chx-2-ATT	$5.34\cdot10^{-8}$	16.523±0.423	0.621±0.002	65.63±0.48	6.80±0.12

Experimental conditions: 6 µm thick anodes of Dyesol 18NR-AO (paste). 0.1 mM THF dye solution, 5 h immersion.

Regarding the amount of sensitizer adsorbed on the photoanode, the highest value ($4.33\cdot10^{-7}$ mol/cm^2) has been obtained by **AT-SIL** while the lowest value has been reached by dianchored **Chx-2-AT** ($1.06\cdot10^{-7}$ mol/cm^2) and **Chx-2-ATT** ($5.34\cdot10^{-8}$ mol/cm^2). In spite of the lowest amount of dibranched sensitizers, the best photovoltaic performance of **Chx-2-ATT-**chromophore-devices notes the promising molecular σ-linkage of this 3-methyl-1,1-cyclohexane derivative with bithiophene.

Finally, the devices performance stability has been carried out and the photovoltaic parameters ($J_{sc,}$ $V_{oc,}$ ff and η) have been studied over time. The results are depicted in **Figure 7** and show that the four studied dyes (**AT-SIL, ATT-SIL, Chx-2-AT** and **Chx-2-ATT**) are stable up to 1040 h after the cell assembly.

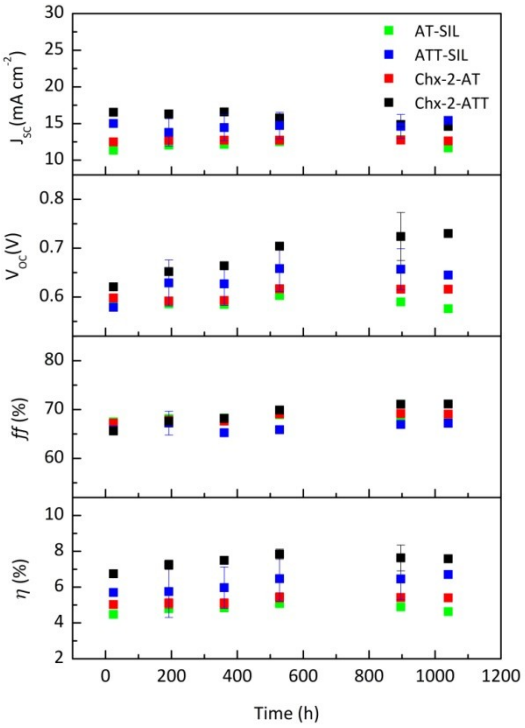

Figure 7. Photovoltaic parameters of devices prepared with dyes **AT-SIL, ATT-SIL, Chx-2-AT** and **Chx-2-ATT** with 6 µm thick anodes and after 5 h of immersion time and measured under the irradiance of AM 1.5 G sunlight (1 sun 1000 W/m^2).

In particular, it is remarkable that V_{oc} and η for devices based on **Chx-2-ATT** show an increase of c.a. 18 and 12 %, respectively (**Table S.1**). The best results obtained in this temporal study were reached 528 h after cell-assembly and these results are shown in (**Table 5** and **Figure S.31**).

Table 5. Average value of the measured photovoltaic parameters: open circuit voltage (V_{oc}), short circuit current density (J_{sc}), fill factor (*ff*) and overall efficiency (η). 528 h after cell assembly. Three cells of each type were prepared and characterized.

Dye	J_{sc} (mA·cm^{-2})	V_{oc} (V)	*ff* (%)	η (%)
AT-SIL	12.51±0.02	0.603±0.004	68.93±0.30	5.08±0.06
ATT-SIL	14.73±1.82	0.658±0.046	65.88±0.21	6.47±1.25
Chx-2-AT	12.73±0.42	0.617±0.005	69.10±0.54	5.43±0.27
Chx-2-ATT	15.76±0.28	0.704±0.007	69.89±0.54	7.84±0.28

Experimental conditions: 6 µm thick electrodes of Dyesol 18NR-AO (paste). 0.1 mM THF dye solution, 5 h immersion.

Electrochemical impedance spectroscopy was carried out in the dark under a bias corresponding to V_{oc} with frequency range of 0.1-100 kHz. In the Nyquist plot *(–Z''* vs *Z'*) the larger semicircle (intermediate frequency range) is related to the charge recombination resistance (R_{rec}) at the TiO_2/dye/electrolyte interface. In previous studies [34-37], when comparing the recombination resistance of different samples it has been found that the higher the value of R_{rec}, the larger the V_{oc}.

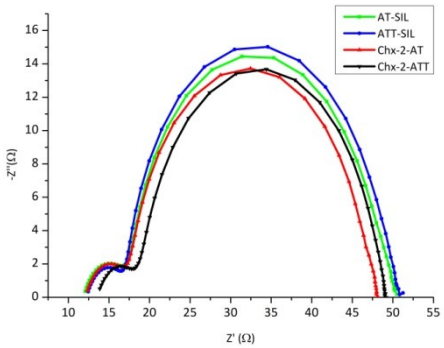

Figure 8. Nyquist plot of devices 6 µm, 5 h immersion time prepared with dyes **AT-SIL, ATT-SIL, Chx-2-AT** and **Chx-2-ATT** in the dark, 528 h after cell-assembly.

The Nyquist plots in **Figure 8,** measured 528 h after the cell-assembly, show semicircles of similar size for the four dyes, with R_{rec} values around 30 Ω. According with that, similar V_{oc} values would be expected. The larger one obtained for **Chx-2-ATT** in *J-V* measurements could be related with the highest current value for the derivative. (**Figure 8**) The facile electron-injection is responsible for the large J_{sc} observed for the device using the **Chx-2-ATT** dye.

3.- Conclusions

Two novel difunctionalized dyes were prepared using 3-methy-1,1-cyclohexane as σ-linkage, a functionalized derivative of *N, N*-dialkylaniline as the donor unit, cyanoacetic acid as an acceptor unit and thiophene derivatives as π spacers. They depicted a remarkable increase of the molar extinction coefficients with respect to the corresponding individual dyes due to the two electronic transitions with very similar excitation energies predicted by TD-DFT, which will allow these difunctionalized sensitizers to work in low light conditions.

The **Chx-2-ATT** dye has a higher absorption than the **Chx-2-AT** dye; fact that we can attribute to the extended conjugation of the π spacer due to the double ring of thiophene which allows a better transfer of electrons between the donor and the acceptor than the spacer π with a single ring of thiophene.

Novel difunctionalized dyes present higher efficiency as compared to that of single D-π-A analogues because of higher V_{oc} and J_{sc} values. In particular, devices based on **Chx-2-ATT** have given rise to an efficiency value of 7.8 % which means an increase of 21 % of the efficiency with respect to the single **ATT-SIL** dye.

Sensitizers **AT-SIL, ATT-SIL, Chx-2-AT** and **Chx-2-ATT** are stable up to 1040 h after the cell assembly.

Further development of the novel σ-linkage could be achieved through appropriate structural modifications. For instance, the incorporation of two different linked chromophores would lead to a broader absorption and, consequently, an improved efficiency would be expected.

4. Experimental Section

4.1. Materials and methods

All reagents were purchased from Merck and used without purification. Solvents were dried through a commercial available solvent purification system.

Compound **1** was prepared according with reported procedure. [25]

5'-(4-((2-((tert-butyldimethylsilyl)oxy)ethyl)(methyl)amino)phenyl)-[2,2'-bithiophene]-5-carbaldehyde 2

4-bromo-*N*-(2-((*tert*-butyldimethylsilyl)oxy)ethyl)-*N*-methylaniline (0.50 g, 1.45 mmol) was solved in THF (30 mL) at -78 ^{o}C of temperature under argon atmosphere. A *n*-butyllithium solution (1.6 M in THF) (1.47 mL, 2.36 mmol) was slowly added and it was stirred for 35 minutes. Next, a tributyltin chloride solution (0.5 mL, 1.74 mmol) was put together and stirred for 5 minutes. After that, it was stirred at room temperature during 150 minutes.

The crude of the reaction was quenched by the addition of 55 mL of diethyl ether and it was washed with brine and dried. After the solvent evaporation under reduced pressure, the organic residue was used directly in the next step.

In a flask with the yellow residue solved in 22 mL of toluene, a solution of 5'-Bromo-[2,2']bithiophenyl-5-carboxaldehyde (317 mg, 1.16 mmol) was added. The mixture was desgassed with argon during 15 minutes. Then $Pd(PPh_3)_4$ (0.087 g, 0.07 mmol) was added and the mixture was refluxed for 24 hours under argon atmosphere. The reaction was quenched by the addition of 66 mL of water. The mixture was extracted with toluene (2 x 60 mL). The organic layer was washed with NH_4Cl (1 x 60 mL) and H_2O (2 x 60 mL), was dried over magnesium sulfate and the solvent was evaporated by reduced pressure. The residue was purified by flash chromatography (hexane/diethyl ether 9:1) and the aldehyde was isolated as red solid (179 mg, 34 %).

Molecular weight (g/mol): 457.72 **Melting point** (°C, at 760 mmHg): 145. **FTIR** (KBr, υ_{max}/cm^{-1}): 1658 (C=O). **^{1}H-NMR** ($CD_3(CO)CD_3$, 300 MHz, 293 K): δ (ppm) 0.03 (s, 6H), 0.88 (s, 9H), 3.07 (s, 3H), 3.57 (t, *J*= 5.7 Hz, 2H), 3.86 (t, *J*= 5.8 Hz, 2H), 6.80 (d, *J*= 8.9 Hz, 2H), 7.27 (d, *J*= 3.9 Hz, 1H), 7.41 (d, *J*= 4.0 Hz, 1H), 7.46 (d, *J*= 3.9 Hz, 1H), 7.53 (d, *J*= 8.9

Hz, 2H), 7.90 (d, *J*= 4.0 Hz, 1H), 9.90 (s, 1H) **^{13}C-NMR** ($CD_3(CO)CD_3$, 100 MHz, 293K): δ (ppm) -5.2, 18.8, 26.2, 39.5, 55.1, 61.4, 113.0, 121.7, 122.7, 124.6, 127.5, 128.5, 139.2, 142.1, 148.3, 150.2, 183.4. **HMRS** (ESI^+) m/z: Found: 457.1545 $[M]^+$; molecular formula $[C_{24}H_{31}NO_2S_2Si]$: 457.1560.

5-(4-((2-hydroxyethyl)(methyl)amino)phenyl)thiophene-2-carbaldehyde 3

Compound **1** (187 mg, 0.50 mmol) was solved in dry THF (20 mL) at temperature of 0°C under argon, and a tetrabutylammonium fluoride solution (1 M THF) (1.00 mL, 1.00 mmol) was slowly added and was stirred for 1 h and 30 min. The solution was quenched by the addition of 55 mL of H_2O and 100 mL of NH_4Cl saturated solution (aq). The aqueous phase was extracted with ethyl acetate solution (3x50 mL) and the organic phase was dried and the solvent was evaporated by reduced pressure. The residue was purified by flash chromatography using hexane/ethyl acetate from (1:1) to yield a red solid (116 mg, 89 %).

Molecular weight (g/mol): 261.34. **Melting point** (°C, at 760 mmHg): 134-136. **^{1}H-NMR** (CD_2Cl_2, 400 MHz, 293 K): δ (ppm) 1.63 (t, 1H), 3.04 (s, 3H), 3.54 (t, *J*= 5.7 Hz, 2H), 3.82 (t, *J*= 5.7 Hz, 2H), 6.79 (d, *J*= 9.0 Hz, 2H), 7.27 (d, *J*= 4.0 Hz, 1H), 7.57 (d, *J*= 9.0 Hz, 2H), 7.69 (d, *J*= 4.0 Hz, 1H) 9.80 (s,1H). **^{13}C-NMR** (CD_2Cl_2, 100 MHz,): δ (ppm) 39.3, 55.2, 60.7, 112.8, 121.5, 122.2, 128.0, 138.6, 140.8, 151.3, 156.1, 182.9. **HMRS** (ESI^+) m/z: Found: 284.0727 $[M+Na]^+$; calculated $[C_{14}H_{15}NO_2SNa]$: 284.0716.

5'-(4-((2-hydroxyethyl)(methyl)amino)phenyl)-[2,2'-bithiophene]-5-carbaldehyde 4

Compound **2** (167 mg, 0.37 mmol) was solved in dry THF (20 mL) at temperature of 0°C under argon, a tetrabutylammonium fluoride solution (1 M THF) (73 µL, 0.73 mmol)

was slowly added and was stirred for 1h and 30 min. The solution was quenched by the addition of 55 mL of H_2O and 100 mL of NH_4Cl saturated solution (aq). The aqueous phase was extracted with ethyl acetate solution (3x50 mL) and the organic phase was dried and the solvent was evaporated by reduced pressure. The residue was purified by flash chromatography using hexane/ethyl acetate from (1:1) to yield a red solid (112 mg, 73 %).

Molecular weight (g/mol): 343.46. **Melting point** (°C, at 760 mmHg): 187. **FTIR** (KBr, υ_{max}/cm^{-1}): 1652 (C=O), 3480 (O-H). **^{1}H-NMR** (DMSO-d_6, 400 MHz, 293 K): δ (ppm) 2.98 (s, 3H), 3.44 (t, *J*= 5.8 Hz, 2H), 3.56 (c, *J*= 5.8 Hz, 2H), 4.72 (t, 1H), 6.74 (d, *J*= 8.9 Hz, 2H), 7.33 (d, *J*= 3.9 Hz, 1H), 7.48 (d, *J*= 4.0 Hz, 1H), 7.50 (d, *J*= 8.9 Hz, 2H), 7.54 (d, *J*= 3.9 Hz, 1H), 7.98 (d, *J*= 4.0 Hz, 1H), 9.86 (s, 1H). **^{13}C-NMR** (DMSO-d_6, 100 MHz, 293K): δ (ppm) 38.6, 54.0, 58.1, 111.8, 120.0, 122.1, 124.3, 126.5, 128.3, 131.3, 139.4, 140.4, 146.1, 146.8, 149.3, 183.6. **HMRS** (ESI^+) m/z: Found: 709.1289 $[2M+Na]^+$; calculated $[C_{36}H_{34}N_2NaO_4S_4]$: 709.1293.

ATT-SIL

Aldehyde **2** (100 mg, 0.22 mmol) and 2-cyanoacetic acid (28.1 mg, 0.33 mmol) were solved in chloroform (10 mL) and piperidine (149 µL, 1.45 mmol). The mixture was heated to 65 ^oC of temperature for 24 h under argon atmosphere and prevented from light, and then it was cooled down to room temperature. The mixture was acidified with HCl 0.1 M (18 mL) and extracted with dichloromethane (2 x 50 mL). The organic layer was washed with water (3 x 50 mL), dried and the solvent was evaporated by reduced pressure. The resulting solid was triturated with cold diethyl ether. The final product was isolated as dark purple solid (16 mg, 14 %).

Molecular weight (g/mol): 524.77. **Melting point** (°C, at 760 mmHg): 200. **FTIR** (KBr, υ_{max}/cm^{-1}): 1682 (C=O), 2220 (CΞN), 3395 (O-H). **^{1}H-NMR** (DMSO-d_6, 400 MHz, 293 K) δ (ppm): 0.02 (s, 6H), 0.83 (s, 9H), 2.98 (s, 3H), 3.50 (t, *J*= 5.5 Hz, 2H), 3.75 (t, *J*= 5.5 Hz, 2H), 6.74 (d, *J*= 9.0 Hz, 2H), 7.35 (d, *J*= 4.0 Hz, 1H), 7.49-7.55 (m, 4H), 7.90 (d, *J*= 4.0 Hz, 1H), 8.38 (s, 1H). **^{13}C-NMR** (DMSO-d6, 100 MHz, 293 K) δ (ppm): -5.4, 17.9, 25.8, 38.9, 53.7, 60.2, 111.9, 117.3, 120.1, 122.3, 124.0, 126.5, 128.1, 131.4, 133.6, 146.8, 149.2, 159,2 163.6. **HMRS** [ESI]$^{+}$ m/z: Found 524.1644 [M]$^{+}$; calculated [$C_{27}H_{32}N_2O_3S_2Si$]: 524.1618.

bis(2-((4-(5-formylthiophen-2-yl)phenyl)(methyl)amino)ethyl) 2,2'-(3-methylcyclohexane-1,1-diyl)diacetate 5

3-methyl-1,1-cyclohexanediacetic acid (45 mg, 0.21 mmol) was solved in 3 mL of THF and 4-dimethylaminopyridine (DMAP) (22 mg, 0.18 mmol) and 1-ethyl-3-[3-dimethylaminopropyl]carbodiimide hydrochloride (EDC) (242 mg, 1.26 mmol) were successively added. This mixture was maintained at temperature of 0 °C during 30 min. Alcohol **3** (110 mg, 0.42 mmol) was added. The reaction mixture was then stirred at room temperature for 7 days. Then it was washed and dried and the solvent was evaporated by reduced pressure. The residue was purified by flash chromatography using hexane/ethyl acetate from (1:1) to yield a yellow solid (71 mg, 48 %).

Molecular weight (g/mol): 700.91. **FTIR** (NaCl, υ_{max}/cm^{-1}): 1377 (C-O), 1444 (C-O), 1605 (C=O), 1657 (C=O), 1733 (C=O). **^{1}H-NMR** (CD_2Cl_2, 400 MHz, 293 K): δ (ppm) 0.65-0.75 (m, 1H), 0.79 (d, *J*= 6.4 Hz, 3H), 1.01-1.12 (m, 1H), 1.31-1.50 (m, 4H), 1.60-1.70 (m, 3H), 2.38 (s, 2H), 2.53 (s, 2H), 3.01 (s, 3H), 3.01 (s, 3H), 3.61 (t, *J*= 6.0 Hz, 2H), 3.61 (t, *J*= 6.0 Hz, 2H), 4.21 (t, *J*= 6.0 Hz, 2H), 4.21 (t, *J*= 6.0 Hz, 2H), 6.74 (d, *J*= 9.0 Hz, 4H), 7.25 (d, *J*=

4.0 Hz, 2H), 7.55 (d, *J*= 9.0 Hz, 4H), 7.68 (d, *J*= 4.0 Hz, 1H), 7.68 (d, *J*= 4.0 Hz, 1H), 9.79 (s, 1H), 9.80 (s, 1H) **^{13}C-NMR** (CD_2Cl_2, 100 MHz, 293K): δ (ppm) 22.08, 23.12, 27.92, 35.13, 35.72, 36.30, 37.76, 39.02, 39.06, 44.99, 45.89, 51.27, 61.42, 61.46, 112.57, 112.59, 121.47, 122.14, 128.02, 128.03, 138.64, 150.51, 155.77, 172.06, 172.48, 182.84. **HMRS** (ESI^+) m/z: Found: 723.2514 $[M+Na]^+$; calculated $[C_{39}H_{44}N_2NaO_6S_2]$: 723.2533.

bis(2-((4-(5'-formyl-[2,2'-bithiophen]-5-yl)phenyl)(methyl)amino)ethyl) 2,2'-(3-methylcyclohexane-1,1-diyl)diacetate 6

3-methyl-1,1-cyclohexanediacetic acid (35 mg, 0.16 mmol) was solved in 3 mL of DMF and 4-dimethylaminopyridine (DMAP) (36 mg, 0.29 mmol) and 1-ethyl-3-[3-dimethylaminopropyl]carbodiimide hydrochloride (EDC) (452 mg, 2.36 mmol) were successively added. This mixture was maintained at temperature of 0 °C during 30 min. Alcohol **4** (112 mg, 0.33 mmol) was added. The reaction mixture was then stirred at room temperature for 3 days. The aqueous phase was extracted with CH_2Cl_2 (3x50 mL) and washed with H_2O (3x50 mL). The organic phase was dried and the solvent was evaporated by reduced pressure. The residue was purified by flash chromatography using /toluene/ethyl acetate/NEt_3 from (8:2:0.0025) to yield a yellow solid (60 mg, 42 %).

Molecular weight (g/mol): 865.15 **Melting point** (°C, at 760 mmHg)**:** 122 (D). **FTIR** (KBr, υ_{max}/cm^{-1}): 1457 (C-O), 1606 (C=O), 1659 (C=O), 1735 (C=O). **^{1}H-NMR** (CD_2Cl_2, 400 MHz, 293 K): δ (ppm) 0.68-0.78 (m, 1H), 0.81 (d, *J*= 6.4 Hz, 3H), 1.05-1.12 (m, 1H), 1.25-1.55 (m, 4H),1.58-1.75 (m, 3H),2.40 (s, 2H), 2.55 (s, 2H), 2.99 (s, 3H), 3.00 (s, 3H), 3.60 (t, *J*=

5.5 Hz, 2H), 3.60 (t, *J*= 5.5 Hz, 2H), 4.21 (t, *J*= 5.5 Hz, 2H), 4.21 (t, *J*= 5.5 Hz, 2H), 6.73 (d, *J*= 9.0 Hz, 4H), 7.10 (d, *J*= 3.8 Hz, 2H), 7.22 (d, *J*= 4.0 Hz, 2H), 7.30 (d, *J*= 3.8 Hz, 2H), 7.47 (d, *J*= 9.0 Hz, 4H), 7.66 (d, *J*=4.0 Hz, 2H), 9.82 (s, 2H). **^{13}C-NMR** (CD_2Cl_2, 100 MHz, 293K): δ (ppm) 22.12, 23.15, 27.95, 35.17, 35.76, 36.33, 37.84, 39.03, 39.06, 45.04, 45.96, 51.40, 61.51, 61.55, 112.71, 112.73, 122.14, 122.32, 123.17, 124.03, 127.34, 127.35, 127.86, 133.24, 138.15, 141.58, 147.96, 149.71, 170.08, 172.50, 182.84. **HMRS** (ESI^+) m/z: Found: 887.2267 $[M+Na]^+$; calculated $[C_{47}H_{48}N_2NaO_6S_4]$: 887.2287.

Dye Chx-2-AT

Dialdehyde **5** (68 mg, 0.10 mmol) and 2-cyanoacetic acid (25 mg, 0.29 mmol) were solved in chloroform (10 mL) and piperidine (130 µL, 1.28 mmol). The mixture was heated to 65°C of temperature for 24 hours under argon atmosphere and prevented from light; then it was cooled down to room temperature. The mixture was acidified with HCl 0.1 M (9 mL) and extracted with dichloromethane (3 x 50 mL). The organic layer was washed with water (4 x 50 mL), dried and the solvent was evaporated by reduced pressure. The resulting solid was triturated with cold methanol. The final product was isolated as black solid (48 mg, 59 %).

Molecular weight (g/mol): 835.00 **Melting point** (°C, at 760 mmHg)**:** 167 (D). **FTIR** (KBr, υ_{max}/cm^{-1}): 1195 (C-O), 1217 (C-O), 1378 (C=O), 1415 (C=O), 1568 (C=O); 1606 (C=O), 2214 (C≡N), 3408 (O-H). **^{1}H-NMR** (DMSO-d_6, 400 MHz, 293 K): δ (ppm) 0.50-0.62 (m, 1H), 0.69 (d, *J*= 6.2 Hz, 3H), 0.92-1.02 (m, 1H), 1.15-1.42 (m, 4H), 1.42-1.56 (m, 3H), 2.25 (s, 2H), 2.38 (s, 2H), 2.94 (s, 3H), 2.95 (s, 3H), 3.62 (brt, 4H) 4.15 (brt, 2H), 4.16 (brt, 2H), 6.76 (d, *J*= 8.9 Hz, 4H), 7.49 (d, *J*= 3.8 Hz, 2H), 7.56 (d, *J*= 8.9 Hz, 4H), 7.87 (d, *J*= 3.8 Hz, 2H), 8.33 (s, 2H) **^{13}C-NMR** (DMSO-d_6, 100 MHz, 293K): δ (ppm): 61.0, 112.2,

118.0, 120.1, 125.9, 127.2, 127.3, 132.6, 133.6, 142.1, 144.5, 149.8, 149.9, 164.5, 171.0, 171.4. **HMRS** (ESI^-) m/z: Found: 833.2646 $[M-H]^-$, calculated $[C_{45}H_{45}N_4O_8S_2]$: 833.2684.

Dye Chx-2-ATT

Dialdehyde **6** (58 mg, 0.07 mmol) and 2-cyanoacetic acid (17 mg, 0.20 mmol) were solved in chloroform (10 mL) and piperidine (90 µL, 0.88 mmol). The mixture was heated to 65°C of temperature for 24 hours under argon atmosphere and prevented from light; then it was cooled down to room temperature. The mixture was acidified with HCl 0.1 M (3 mL) and extracted with dichloromethane (3 x 50 mL). The organic layer was washed with water (4 x 50 mL), dried and the solvent was evaporated by reduced pressure. The resulting solid was triturated with cold methanol. The final product was isolated as black solid (34 mg, 51 %).

Molecular weight (g/mol): 999.25. **Melting point** (°C, at 760 mmHg)**:** 194. **FTIR** (KBr, υ_{max}/cm^{-1}): 1155 (C-O), 1210 (C-O), 1414 (C=O), 1440 (C=O) 1578 (C=O), 1608 (C=O), 2214(C≡N), 3439 (O-H). **^{1}H-NMR** (DMSO-d_6, 400 MHz, 293 K): δ (ppm) 0.56-0.67 (m, 1H), 0.71 (d, *J*= 6.2 Hz, 3H), 0.68-0.75 (m, 1H), 0.96-1.04 (m, 1H), 1.22-1.29 (m, 1H), 1.32-1.39 (m, 2H), 1.48-1.51 (m, 1H), 1.54-1.57 (m, 2H) 2.27 (s, 2H), 2.40 (s, 2H), 2.92 (s, 3H), 2.93 (s, 3H), 3.58-3.61 (m, 4H), 4.3-4.16 (m, 4H), 6.73 (d, *J*= 8.5 Hz, 4H), 7.31 (d, *J*= 3.7 Hz, 1H), 7.32 (d, *J*= 3.7 Hz, 1H), 7.47 (d, *J*= 4.1 Hz, 2H), 7.48 (d, *J*= 8.5 Hz, 4H), 7.51 (d, *J*= 3.7 Hz, 2H), 7.90 (d, *J*= 4.1 Hz, 2H), 8.40 (s, 2H). **^{13}C-NMR** (DMSO-d_6, 75 MHz, 293K): δ (ppm) 21.0, 21.7, 22.2, 22.7, 26.7, 34.2, 34.4, 35.3, 37.0, 38.1, 38.2, 43.7, 44.8, 50.0, 60.9, 61.0, 91.9, 98.2, 112.1, 116.9, 120.5, 122.4, 124.1, 126.5, 126.6, 128.3,

131.5, 133.3, 141.2, 146.0, 146.9, 149.0, 163.7, 170.9, 171.4. **HMRS** (ESI^+) m/z: Found: 999.2587 $[M+H]^+$; calculated $[C_{53}H_{51}N_4O_8S_4]$: 999.2584.

Acknowledgements

We gratefully acknowledge the financial support from the Universidad de Zaragoza (UZ2019-CIE-01), the Spanish Ministry of Science and Innovation-MICINN-FEDER (Project CTQ2014–52331-R) and Gobierno de Aragón-Fondo Social Europeo (E14-17R). ID and DB acknowledge for the financial support of DGA fellowship and PhD studentship Santander-2018 programs, respectively.

References

[1] O'Regan B, Grätzel M. A low-cost, high-efficiency solar cell based on dye-sensitized colloidal TiO_2 films. Nature 1991; 353: 737–40. https://doi.org/10.1038/353737a0

[2] Hagfeldt A, Boschloo G, Sun LC, Kloo L, Pettersson H. Dye-sensitized solar cells. Chem Rev 2010; 110: 6595-663. http://dx.doi.org/10.1021/cr900356p

[3] Hardin BE, Snaith HJ, McGehee M. The renaissance of dye-sensitized solar cells. Nat Phot 2012; 6: 162-9. http://dx.doi.org/10.1038/nphoton.2012.22

[4] De Sousa S, Lyu S, Ducasse L, Toupance T, Olivier C. Tuning visible-light absorption properties of Ru– diacetylide complexes: simple access to colorful efficient dyes for DSSC. J Mater Chem A, 2015; 3: 18256–64. http://dx.doi: 10.1039/C5TA04498G

[5] Ji M, Zhou H, Kim H-K. Rational design criteria for D–p–A structured organic and porphyrin sensitizers for highly efficient dye-sensitized solar cells. J Mater Chem A, 2018; 6: 14518–45. http://dx.doi: 10.1039/C8TA02281J

[6] Mishra A, Fischer MK, Bauerle P. Metal-Free Organic Dyes for Dye-Sensitized Solar Cells: From Structure: Property Relationships to Design Rules. Angew Chem, Int Ed 2009; 48: 2474-99. http://dx.doi: 10.1002/anie.200804709

[7] Ooyama Y, Harima Y. Molecular Designs and Syntheses of Organic Dyes for Dye-Sensitized Solar Cells. Eur J Org Chem 2009, 2903-34. https://doi.org/10.1002/ejoc.200900236

[8] Liang M, Chen J. Arylamine organic dyes for dye-sensitized solar cells. Chem Soc Rev 2013; 42: 3453-88. http://dx.doi.org/10.1039/c3cs35372a

[9] Dong L, Chen R, Weng Q, An Z, Chen X, Chen P. The effect of furan linkers on the properties of cyclic thiourea functionalized triphenylamine dye sensitizers. Dyes Pigm 2017; 139: 772-8. http://dx.doi.org/10.1016/j.dyepig.2017.01.014 0143-7208

[10] Paramasivarn M, Chitumalla RK, Singh SP, Islam A, Han L, Rao VJ, Bhanuprakash K. Tuning the photovoltaic performance of benzocarbazole-based sensitizers for dye-sensitized solar cells: a joint experimental and theoretical study of the influence of π-spacers. J Phys Chem C 2015; 119: 17053-64. http://dx.doi.org/10.1021/acs.jpcc.5b04629

[11] Eom YK, Kang SH, Choi IT, Yoo Y, Kim J, Kim H. Significant light absorption enhancement by a single heterocyclic unit change in the p-bridge moiety from thieno[3,2-b]benzothiophene to thieno[3,2-b]indole for high performance dyesensitized and tandem solar cells. J Mater Chem A, 2017; 5: 2297–308. http://dx.doi.org/10.1039/C6TA09836C

[12] Zhu S, An Z, Chen X, Chen P, Liu Q. Cyclic thiourea functionalized dyes with binary π-linkers: Influence of different π-conjugation segments on the performance of dye-

sensitized solar cells Dyes Pigm 2015; 116: 146-54. http://dx.doi.org/10.1016/j.dyepig.2015.01.022

[13] Jia H, Ju X, Zhang M, Ju Z, Zheng H. Heterocycle Containing Different Atoms as π-bridge effect on the Performance of Dye-Sensitized Solar Cells. Phys Chem Chem Phys 2015; 17: 16334-40. http://dx.doi.org/10.1039/C5CP02194D

[14] Chen R, Yang X, Tian H, Wang X, Hagfeldt A, Sun L. Effect of Tetrahydroquinoline Dyes Structure on the Performance of Organic Dye-Sensitized Solar Cells Chem Mater 2007; 19: 4007-15. https://doi.org/10.1021/cm070617g

[15] Zhu W, Wu Y, Wang S, Li W, Li X, Chen J, Wang ZS, Tian H. Organic D-A- π -A Solar Cell Sensitizers with Improved Stability and Spectral Response Adv Funct Mater, 2011; 21: 756-63. http://dx.doi.org/10.1002/adfm.201001801

[16] Wu Z-S, Guo W-J, Zhang J, Liu YD, Song X-C, Jiang Y, Weng Q, An ZW. Novel 4,4'-bis(alkylphenyl/alkyloxyphenyl)-2,2'-bithiophene bridged cyclic thiourea functionalized triphenylamine sensitizers for efficient dyesensitized solar cells. Solar Energy, 2019; 186: 1-8. http://dx.doi.org/10.1016/j.solener.2019.04.090

[17] Seo KD, You BS, Choi IT, Ju MJ, You M, Kang HS, Kim HK. Dye-Sensitized Solar Cells based on Organic Dual-Channel Anchorable Dyes with Well-Defined Core Bridge Structures. *ChemSusChem* 2013; 6: 2069-73. https://doi.org/10.1002/cssc.201300365

[18] Kumar D, Wong KT. Mater. Organic dianchor dyes for dye-sensitized solar cells. Today Energy, 2017; 5: 243-79. https://doi.org/10.1016/j.mtener.2017.05.007

[19] Baheti A, Justin Thomas KR, Lin LC, Lee KM. Monoanchoring (D-D-π-A) and Dianchoring (D-D-$(\pi\text{-A})_2$) Organic Dyes Featuring Triarylamine Donors Composed of

Fluorene and Carbazole. Asian J Org Chem 2014; 3: 886-98. https://doi.org/10.1002/ajoc.201402073

[20] Tan LL, Liu JM, Li SY, Xiao LM, Kuang DB, Su CY. Dye-sensitized solar cells with improved performance using cone-calix[4]arene based dyes. ChemSusChem 2015; 8: 280-7. https://doi.org/10.1002/cssc.201402401

[21] Lin R Y-Y, Wu F-L, Chang C-H, Chou H-H, Chuang TM, Chu T-C, Hsu C-Y, Chen P-W, Ho K-C, Lo Y-H, Lin J-T. Y-shaped metal-free D–π–$(A)_2$ sensitizers for high-performance dye-sensitized solar cells. J Mater Chem A, 2014; 2: 3092-101. http://dx.doi.org/10.1039/C3TA14404F

[22] Andreu R, Franco S, Garín J, Romero J, Villacampa B, Blesa MJ, Orduna J, Multichromophoric calix[4]arenes: Effect of interchromophore distances on linear and nonlinear optical properties. ChemPhysChem 2012; 13: 3204–9. https://doi.org/10.1002/cphc.201200203

[23] Castillo-Vallés M, Andrés-Castán JM, Garín J, Orduna J, Villacampa B, Franco S, Blesa MJ. Dye-sensitized-solar-cells based on calix[4]arene scaffolds. RSC Adv 2015; 5: 90667–70. https://doi.org/10.1039/c5ra15184h

[24] Colom E, Andrés-Castán JM, Barrios D, Duerto I, Franco S, Garín J, Orduna J, Villacampa B, Blesa MJ. Modification of the electronic properties of the π-spacer of chromophores linked to calix[4]arene platform for DSSCs applications. Dyes Pigm 2019; 164: 43–53. https://doi.org/10.1016/j.dyepig.2018.12.066

[25] Duerto I, Colom E, Andrés JM,Franco S, Garín J, Orduna J, Villacampa B, Blesa MJ. DSSCs based on aniline derivatives functionalized with a tert-butyldimethylsilyl group and the effect of the π–spacer. Dyes Pigm 2018; 148: 61-71. http://dx.doi.org/10.1016/j.dyepig.2017.07.063C2CC33921H

[26] Zhu L, Yang Y, Zhang D, Du Z; Bao B, Lin Q, Chen X, Yang L, Bao C, Ge Y. PCT Int. Apl.(2018), WO 2018014821 A1 20180125. Language: Chinese, Database: CAPLUS.

[27] Amro K, Daniel J, Clermont G, Bsaibess T, Pucheault M, Genin E, Vaultier M, Blanchard-Desce M. A new route towards fluorescent organic nanoparticles with red-shifted emission and increased colloidal stability. Tetrahedron 2014; 70: 1903-9. DOI: 10.1016/j.tet.2014.01.032

[28] Leliege A, Le Regent CH, Allain M, Blanchard P, Roncali J. Structural modulation of internal charge transfer in small molecular donors for organic solar cells. Chem Commun 2012; 48: 8907-9. http://dx.doi.org/10.1039/C2CC33921H.

[29] Nüesch F, Grätzel M. *H*-aggregation and correlated absorption and emission of a merocyanine dye in solution, at the surface and in the solid state. A link between crystal structure and photophysical properties. Chem Phys 1995; 193: 1–17, http://dx.doi.org/10.1016/0301-0104(94)00405-Y

[30] Hagfeldt A, Grätzel M. Light-Induced Redox Reactions in Nanocrystalline Systems Chem. Rev. 1995; 95: 49–68. https://doi.org/10.1021/cr00033a003

[31] Pazoki M, Cappel UB, Johansson EMJ, Hagfeldt A, Boschloo G. Light-Induced Redox Reactions in Nanocrystalline Systems. Energy Environ Sci 2017; 10: 672–709. https://doi.org/10.1039/c6ee02732f

[32] Wu Y, Zhu W. Organic sensitizers from D–π–A to D–A–π–A: effect of the internal electron-withdrawing units on molecular absorption, energy levels and photovoltaic performances. Chem Soc Rev 2013; 42: 2039-58. http://dx.doi.org/10.1039/C2CS35346F

[33] Zhou G, Pscirer N, Schoneboom JC, Eickemeyer F, Baumgarten M, Mullen K. Ladder-type pentaphenylene dyes for dye-sensitized solar cells. Chem Mater 2008; 20: 1808-15. http://dx.doi.org/10.1021/cm703459p.

[34] Fabregat-Santiago F, Garcia-Belmonte G, Mora-Sero I, Bisquert J. Characterization of nanostructured hybrid and organic solar cells by impedance spectroscopy. Phys Chem Chem Phys 2011; 13: 9083–118. http://dx.doi.org/10.1039/c0cp02249g

[35] Barea EM, Ortiz J, Payá FJ, Fernández-Lázaro F, Fabregat-Santiago F, Sastre-Santos A, Bisquert J. Energetic factors governing injection, regeneration and recombination in dye solar cells with phthalocyanine sensitizers. Energy Environ Sci, 2010; 3: 1985–94. http://dx.doi.org/10.1039/C0EE00185F

[36] Barea EM, Zafer C, Gultekin B, Aydin B, Koyuncu S, Icli S, Fabregat-Santiago F, Bisquert J. Quantification of the Effects of Recombination and Injection in the Performance of Dye-Sensitized Solar Cells Based on N-Substituted Carbazole Dyes. J Phys Chem C, 2010; 114: 19840–8. http://dx.doi.org/10.1021/jp1055842

[37] Barea EM, González-Pedro V, Ripollés-Sanchis T, Wu H-P, Li L-L, Yeh C-Y, Diau E W-G, Bisquert J. Porphyrin Dyes with High Injection and Low Recombination for Highly Efficient Mesoscopic Dye-Sensitized Solar Cells. J Phys Chem C, 2011; 115: 10898–902. http://dx.doi.org/10.1021/jp2018378